International Journal of Physical Sciences Vol. 7(15), pp. 2274 - 2281, 9 April, 2012
Available online at http://www.academicjournals.org/IJPS
DOI: 10.5897/IJPS11.1523
ISSN 1992 - 1950 ©2012 Academic Journals

Full Length Research Paper

Process analysis of electroless copper plating for AB_5-type hydrogen storage alloy using support vector regression

S. Zhao, C. Z. Cai* and J. L. Tang

Department of Applied Physics, Chongqing University, Chongqing 401331, P.R. China.

Accepted 6 March, 2012

Surface modification is an effective method to improve the electrochemical property of hydrogen storage alloy. In order to investigate the influence of process factors of electroless copper (Cu) plating for AB_5-type hydrogen storage alloy on Cu coating mass, a novel modeling approach, support vector regression (SVR) combined with particle swarm optimization (PSO), was proposed to construct a mathematical model for prediction of the mass changes of Cu coating over the AB_5 hydrogen storage alloy surface based on three factors, including temperature, pH value and Ni^{2+} concentration. The modeling accuracy and reliability of the created SVR model are validated through leave-one-out cross validation (LOOCV), and compared with those of a second-order polynomial model. The results show that the predicted errors by SVR-LOOCV models are all smaller than those achieved by the second-order polynomial model. The SVR model is further applied to predict the process parameters for the maximum Cu coating mass. These studies suggest that SVR can be used as an effective methodology to assist the design of experiment, and is helpful to precisely control the coating mass via fine adjustment of the process parameters.

Key words: Surface modification, electroless copper plating, hydrogen storage alloy, support vector regression, modeling and prediction.

INTRODUCTION

Hydrogen as a renewable and non-contamination fuel has continually received much attention. In order to make the hydrogen practical application, storage technologies must be improved to solve the mass storage for transport. AB_5-based hydrogen storage alloy, which exhibits some excellent properties, including fast reversible sorption kinetics with small hysteresis and good cycling life (Schlapbach and Zuttel, 2001; Singh et al., 2007), has been investigated extensively and become large-scale commodity production as negative electrode of the nickel-metal hydride battery (Tliha et al., 2007; Hu and Noreus, 2010; Ozaki et al., 2007; Thomas et al., 2008; Malinova and Guo, 2004; Dong et al., 2010; Zhang et al., 2007). Due to oxidation at the surface during repeated charge-discharge cycling, surface segregation and decomposition of hydrogen storage alloy may cause the electrochemical property of metal hydride electrodes degradation (Lei et al.,1991). To improve the electrochemical property of hydrogen storage alloy electrode in nickel-metal hydride battery, several types of surface modification have been studied in recent literatures. Surface modification for hydrogen storage alloy, which covers the intermetallic powder to prevent corrosion or oxidation, is an effective strategy to improve nickel-metal hydride battery performance (Matsuoka et al., 1993; Yan et al., 1995; Shen et al., 2010; Yu et al., 2009; Raju et al., 2009; Deng et al., 2006). Feng and Northwood (2004) studied the electrochemical properties of metal hydride (MH) electrode micro-encapsulated Cu, which showed higher exchange current density and apparent activation energy when compared with untreated ones. Wei et al. (2008) revealed that the Cu coating of Co-free alloy $La(NiMnAlFe)_5$ increased the maximum discharge capacity

*Corresponding author. E-mail: caiczh@gmail.com. Tel: +86-13996438540.

from 282 to 307 mAh/g, and also enhanced its high-rate discharge ability and cycle life. Zhang et al. (2010) investigated the influence of experimental process on Cu coating mass of electroless copper plating, and found out that the coating mass has obvious effects on the discharge capacity and cycle stability. Therefore, controlling the experimental parameters within a suitable range to achieve the optimal coating mass is becoming more and more significant in the process of electroless copper plating for enhancing the performance of hydrogen storage alloy. Since the electroless copper plating is a complex process, and is greatly influenced by two or more factors simultaneously, the conventional "change-one-factor-at-a-time" method is not appropriate for copper plating experimental design. Orthogonal experimental design combined with mathematic model is an effective methodology to explore variation law of alloy coating. In this study, motivated by Zhang's previous work, a novel computational strategy, using support vector regression (SVR) (Vapnik, 1995) combined with particle swarm optimization (PSO) (Kennedy and Eberhart, 1995) was proposed to analyze the effect of the experimental parameters (temperature, pH value and Ni^{2+} concentration) on the mass change of the electroless Cu coating over the hydrogen storage alloy.

MATERIALS AND METHODS

Theory of support vector regression

Support vector machine (SVM) is a statistical learning approach based on structural risk minimization principle, which was proposed and developed by Vapnik and co-worker (1995). It has been successfully used for classification or regression in real applications (Cai et al., 2003a, b; Wen et al., 2009; Wang et al., 2011). The basic idea of SVR is to map the $\boldsymbol{x}$ into a higher-dimensional feature space F via a nonlinear mapping $\Phi(\boldsymbol{x})$, and then to perform a linear regression in this space. Therefore, SVR is to find the linear relation Equation 1 based on a given training dataset $(\boldsymbol{x}_1, y_1)$, …, $(\boldsymbol{x}_n, y_n)$.

$$f(\boldsymbol{x}) = \boldsymbol{w}\cdot\boldsymbol{\Phi}(\boldsymbol{x}) + b, \boldsymbol{\Phi}: R^{\mathrm{N}} \to \boldsymbol{F}, \boldsymbol{w} \in \boldsymbol{F}, \tag{1}$$

where w is a vector for regression coefficients and b is a bias. They are estimated by minimizing the regularized risk function $R(C)$:

$$R(C) = \frac{1}{2}\|\boldsymbol{w}\|^2 + C\sum_{i=1}^{n} L_{\varepsilon}(f(\boldsymbol{x}_i) - y_i), \tag{2}$$

$$L_{\varepsilon}(f(\boldsymbol{x}_i) - y_i) = \begin{cases} 0, & \text{if } |f(\boldsymbol{x}_i) - y_i| < \varepsilon, \\ |f(\boldsymbol{x}_i) - y_i| - \varepsilon, & \text{if } |f(\boldsymbol{x}_i) - y_i| \geq \varepsilon, \end{cases} \tag{3}$$

where n is the number of training samples, C is a penalty factor, ε is a prescribed parameter controlling the tolerance to error. $(1/2)\|\boldsymbol{w}\|^2$ is used as a flatness measurement of Equation 1. The second term, $C\sum_{i=1}^{n} L_{\varepsilon}(f(\boldsymbol{x}_i) - y_i)$, is the so-called empirical risk, which is measured by ε-insensitive loss function $L_{\varepsilon}(f(\boldsymbol{x}_i) - y_i)$.

To get the indices of w and b for Equation 1, build the Lagrange equation:

$$\begin{aligned} L(\boldsymbol{w}, \xi_i, \xi_i^*) = {} & \frac{1}{2}\|\boldsymbol{w}\|^2 + C\sum_{i=1}^{n}(\xi_i + \xi_i^*) \\ & - \sum_{i=1}^{n}\alpha_i((\varepsilon + \xi_i) + y_i + (\boldsymbol{w}\cdot\Phi(\boldsymbol{x}_i)) + b) \\ & - \sum_{i=1}^{n}\alpha_i^*((\varepsilon + \xi_i^*) + y_i + (\boldsymbol{w}\cdot\Phi(\boldsymbol{x}_i)) + b) \\ & - \sum_{i=1}^{n}(\lambda_i\xi_i + \lambda_i^*\xi_i^*), \end{aligned} \tag{4}$$

where α_i and α_i^* are Lagrange multipliers to be solved. Only the nonzero values of Lagrange multipliers are useful in construction of the regression line, and their corresponding samples are known as support vectors (SVs). Minimum $L(w, \xi_i, \xi_i^*)$ is obtained by making partial differential coefficients for w, b, ξ_i, ξ_i^* equal to zeros. Finally, the function of SVR is as follows:

$$f(\boldsymbol{x}) = \sum_{i=1}^{l}(\alpha_i - \alpha_i^*)k(\boldsymbol{x}, \boldsymbol{x}_i) + b, \tag{5}$$

where l is the number of SVs and $\boldsymbol{k}(\boldsymbol{x}, \boldsymbol{x}_i) = \boldsymbol{\Phi}(\boldsymbol{x})\cdot\boldsymbol{\Phi}(\boldsymbol{x}_i)$ is a kernel function. In this study, radial basis kernel was adopted as the kernel function:

$$k(\boldsymbol{x}, \boldsymbol{x}_i) = \exp(-\gamma\|\boldsymbol{x} - \boldsymbol{x}_i\|^2). \tag{6}$$

Choosing of SVR parameters with particle swarm optimization

PSO is a population method based on stochastic optimization technique developed by Kennedy and Eberhart (1995), and it is inspired by social behavior of bird flocking or fish schooling. The generalization ability of SVR depends entirely on ε of the ε-insensitive loss function, the penalty constant C and the radial basis kernel function parameter γ. Therefore, it is a key issue to find the optimal parameters (ε, C, γ) for SVR model. In this study, the PSO algorithm is employed to rapidly and efficiently search the optimal parameters (ε, C, γ) for SVR.

According to the PSO theory, a problem can be optimized by iteratively trying to move a specific number of particles in the search space based on mathematical formulae to find the optimal solution. In this study, each of the particle swarm is made up of a parameter vector (ε, C, γ). Suppose in a 3-dimensional space, the ith particle is looked as a point and represented as $\boldsymbol{u}_i = (u_{i1}, u_{i2}, u_{i3})^T$, its velocity is represented as $\boldsymbol{v}_i = (v_{i1}, v_{i2}, v_{i3})^T$, which will be influenced by its local best known position $\boldsymbol{p}_{i\mathrm{best}}$, and the global best position $\boldsymbol{g}_{\mathrm{best}}$. At each iterative process, each particle will transfer its position by tracking its local best value, global best value and its present velocity. Their iterative equations are as follows (Yoshida et al., 2000):

$$\boldsymbol{u}_i(t+1) = \boldsymbol{u}_i(t) + \boldsymbol{v}_i(t+1), \tag{7}$$

$$\begin{aligned} \boldsymbol{v}_i(t+1) = {} & \omega\cdot\boldsymbol{v}_i(t) + c_1\cdot\mathrm{rand}()\cdot(\boldsymbol{p}_{i\mathrm{best}} - \boldsymbol{u}_i(t)) \\ & + c_2\cdot\mathrm{rand}()\cdot(\boldsymbol{g}_{\mathrm{best}} - \boldsymbol{u}_i(t)), \end{aligned} \tag{8}$$

where $\boldsymbol{v}(t)$, $\boldsymbol{v}(t+1)$, $\boldsymbol{u}(t)$ and $\boldsymbol{u}(t+1)$ are, respectively, the speed and position of the present moment and the next moment; rand() is a

Table 1. Measured and calculated electroless Cu coating mass under different experimental parameters.

No.	Experimental parameter			Cu coating mass (g)				
	Temperature (ºC)	pH	Nickel sulfate (g/L)	Exp.	Quadratic model	*APE* (%)	SVR-LOOCV	*APE* (%)
1	65	7.5	1.2	0.424977	0.412501	2.94	0.425028	0.01
2	65	7.5	2.8	0.315097	0.339418	7.72	0.315211	0.04
3	65	9.5	1.2	0.302814	0.316515	4.53	0.303028	0.07
4	65	9.5	2.8	0.311701	0.307297	1.41	0.311958	0.08
5	85	7.5	1.2	0.189247	0.200419	5.90	0.194871	2.97
6	85	7.5	2.8	0.197991	0.191058	3.50	0.207553	4.83
7	85	9.5	1.2	0.212724	0.195171	8.25	0.219449	3.16
8	85	9.5	2.8	0.230432	0.249676	8.35	0.230658	0.10
9	62.85	8.5	2	0.45055	0.435126	3.42	0.421572	6.43
10	87.15	8.5	2	0.274182	0.271281	1.06	0.274113	0.03
11	75	7.285	2	0.24701	0.235750	4.56	0.246707	0.12
12	75	9.715	2	0.220115	0.213049	3.21	0.219765	0.16
13	75	8.5	1.028	0.249371	0.255592	2.49	0.249538	0.07
14	75	8.5	2.972	0.268852	0.244305	9.13	0.268581	0.10
15	75	8.5	2	0.247283	0.275214	11.29	0.258297	4.45

random value between 0 and 1; c_1 and c_2 are both learning factors, normally was set as 2; ω is a weighting factor to accelerate the convergence rate, its value should be automatically regulated with the iterative time of algorithm extending, and defined generally as:

$$\omega = \omega_{\min} + (iter_{\max} - iter) \cdot (\omega_{\max} - \omega_{\min}) / iter_{\max}, \quad (9)$$

where ω_{max} and ω_{min} are the biggest and smallest weighting factors, respectively, commonly set as 0.9 and 0.4, *iter* is the number of current iteration and $iter_{max}$ is the total number of iterations.

In this study, mean absolute percentage error (*MAPE*), which directly reflects the performance of SVR model, is selected as the fitness function:

$$MAPE = \frac{1}{n}\sum_{i=1}^{n}\left|\frac{\hat{y}_i - y_i}{y_i}\right|, \quad (10)$$

where n denotes the number of training samples, y_i represents the actual measured value and $\hat{y}_i$ is the estimated value for the ith training sample.

Dataset, modeling strategy and model evaluation

The experimental dataset used in this study was generated by Zhang et al. (2010), which is listed in Table 1 with a total of 15 samples. Zhang et al. (2010) conducted chemical Cu plating for AB_5-type hydrogen storage alloy via varying various factors, including temperature, pH value and Ni^{2+} concentration. The detailed experimental information can be referred to the work of Zhang et al. (2010).

In the modeling process, the values of the Cu coating mass acted as the dependent variables, while three experimental parameters (temperature, pH value and Ni^{2+} concentration) acted as the independent variables. All the inputs were normalized within a closed interval (-1, 1). The new scaled variables were calculated using the following formula:

$$x' = 2 \times \frac{x - x_{\min}}{x_{\max} - x_{\min}} - 1, \quad (11)$$

where, x is the variable to be scaled, x_{min} is the minimum value of the variable, x_{max} is the maximum value of the variable in the dataset to be scaled and x' is the scaled value.

Leave-one-out cross validation (LOOCV) was adopted to evaluate the prediction performance of SVR models. Besides *MAPE*, the root mean square error (*RMSE*) and correlation coefficient (*R*) were also utilized to evaluate the generalization performance of SVR. They are formulated as follows:

$$RMSE = \sqrt{\frac{1}{n}\sum_{i=1}^{n}(\hat{y}_i - y_i)^2}, \quad (12)$$

$$R = \frac{\sum_{i=1}^{n}(\hat{y}_i - \bar{\hat{y}})(y_i - \bar{y})}{\sqrt{\sum_{i=1}^{n}(\hat{y}_i - \bar{\hat{y}})^2 \cdot \sum_{i=1}^{n}(y_i - \bar{y})^2}}, \quad (13)$$

where $\bar{y}$ represents the mean value of actual measured values, and $\bar{\hat{y}}$ is the mean value of estimated values for all test samples.

RESULTS AND DISCUSSION

Performance comparison between the second-order polynomial model and SVR model

The second-order polynomial modeling is a conventional regression methodology, and has been employed to analysis the experimental data of electroless copper

Table 2. Evaluation results for SVR-LOOCV and quadratic model.

Regression method	*MAPE* (%)	*RMSE* (g)	R^2
SVR-LOOCV	1.51	0.0087	0.996
Quadratic model	5.18	0.0156	0.977

plating by Zhang et al. (2010). The relevant second-order polynomial model refined by us is expressed as follow:

$$y = 3.3338 - 0.1093x_1 + 0.3658x_2 - 0.2178x_3 + 0.000528x_1^2 - 0.0344x_2^2 - 0.0267x_3^2 + 0.0023x_1 \cdot x_2 + 0.002x_1 \cdot x_3 + 0.0199x_2 \cdot x_3, \quad (14)$$

where *y* denotes the Cu coating mass, x_1 represents the temperature (°C), x_2 means the pH value and x_3 is the concentration of nickel sulfate (g/L).

Table 1 also presents the comparison between the experimental value of Cu coating mass and estimated results by the second-order polynomial model and SVR-LOOCV model, respectively. It can be viewed from Table 1 that the absolute percentage errors of 6 out of 15 samples by the model of Equation 14 are greater than 5%, accounting for two-fifths of total samples. On the other hand, except only one sample (#9), the absolute percentage errors of other 14 samples predicted by SVR-LOOCV model are all within the range from 0 to 5%. And the maximum absolute percentage error predicted by SVR-LOOCV model is 6.43%, which is smaller than 11.29% calculated by the model of Equation 14.

Table 2 gives the evaluation results calculated by the second-order polynomial model of Equation 14 and SVR-LOOCV models, respectively. It can be found that the *MAPE* of the second-order polynomial model (5.18%) is greater than that of SVR-LOOCV (1.51%). This demonstrates that the accuracy of the SVR model is much greater than that of the second-order polynomial model. Moreover, the superiority of the SVR-LOOCV model can also be revealed from other two evaluation indices, that is, both *RMSE* and *R* of the SVR-LOOCV model (0.0087 g and 0.996) are better than those of the second-order polynomial model (0.0156 g and 0.977), respectively. These results illustrate that the accuracy and reliability of the constructed SVR model are superior to those of the second-order polynomial model.

All the aforementioned results can be intuitively viewed from Figure 1, which displays the comparison of the measured and estimated values for Cu coating mass by using SVR-LOOCV model and the second-order polynomial model of Equation 14, respectively. Figure 1 shows that the estimated values predicted by SVR-LOOCV are very close to the best-fit line with slope of 1. At first glance, most of the plot points (○) are almost located on this line. In contrast to the results of SVR-LOOCV, the estimated points (■) calculated by the second-order polynomial model deviate significantly from the best-fit line. This indicates in empirical that SVR models can perform strong generation ability.

Statistical analysis for SVR-LOOCV models

Bland and Altman (1986) presented a statistical method for assessing agreement of the mathematic model. According to Bland's theory, it is expected that more than 95% of the differences lie between the limit $(\bar{e} - 2 \cdot \delta_e)$ and $(\bar{e} + 2 \cdot \delta_e)$ if the differences are normally distributed. where $\bar{e}$ denotes the mean value of the difference *e* (= r_p – *r*), r_p represents the predicted value by SVR-LOOCV model, *r* stands for the experiment value and δ_e is the standard deviation of difference *e*. The statistical distribution of differences predicted by SVR-LOOCV models for Cu coating mass is plotted as shown in Figure 2. It can be obtained from Tables 1 and 2 that the mean difference $\bar{e}$ of the SVR-LOOCV models for Cu coating mass is equal to 0.0043 g and the standard deviation δ_e is 0.0087 g. The lower limit of agreement is equal to $(\bar{e} - 2 \cdot \delta_e)$ (= -0.013 g), and the upper limit of agreement is equal to $(\bar{e} + 2 \cdot \delta_e) = (0.022g)$. Thus, it can be seen from Figure 2 that, except only one sample (#9), the differences of the other 14 samples all lie within the limit scope between $(\bar{e} - 2 \cdot \delta_e)$ and $(e + 2 \cdot \delta_e)$. Therefore, the differences of nearly close to 95% samples lie within the limit scope. This indicates that the SVR approach can be employed reliably in the application of modeling and analysis for the Cu coating process.

Influence analysis of multi-process parameters

The created SVR model can also be utilized to analyze the influence of the experimental parameters on Cu coating mass of AB_5-type hydrogen storage alloy. According to the established SVR model, the maximum Cu coating mass (0.45055 g) were searched out under experimental parameters of temperature 62.83°C, pH value 8.5 and Ni^{2+} concentration 1.99 g/L. The three-dimensional profile and two-dimensional contour lines of the Cu coating mass varying with different process factors are illustrated in Figures 3 to 5. Figure 3 shows the interaction effect of pH value and temperature on the Cu coating mass with the Ni^{2+} concentration fixed at its optimal value. Figure 4 illustrates the interaction effect of temperature and Ni^{2+} concentration on Cu coating mass with pH value at their optimal value. The interaction effect of pH value and Ni^{2+} concentration on the Cu coating mass are displayed in Figure 5. They illustrate intuitively the influence of temperature, pH value and Ni^{2+} concentration on the Cu coating mass.

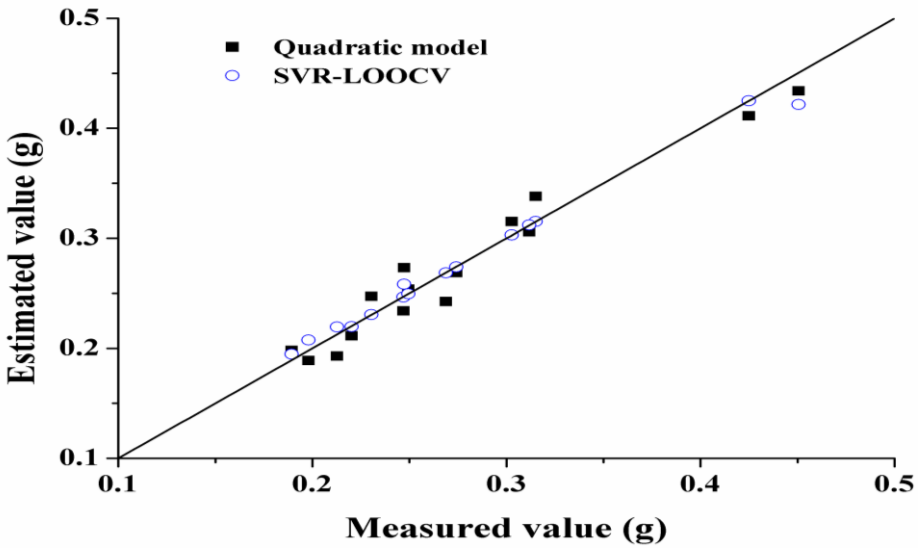

Figure 1. Comparison of experimental and estimated values calculated by SVR-LOOCV and quadratic model.

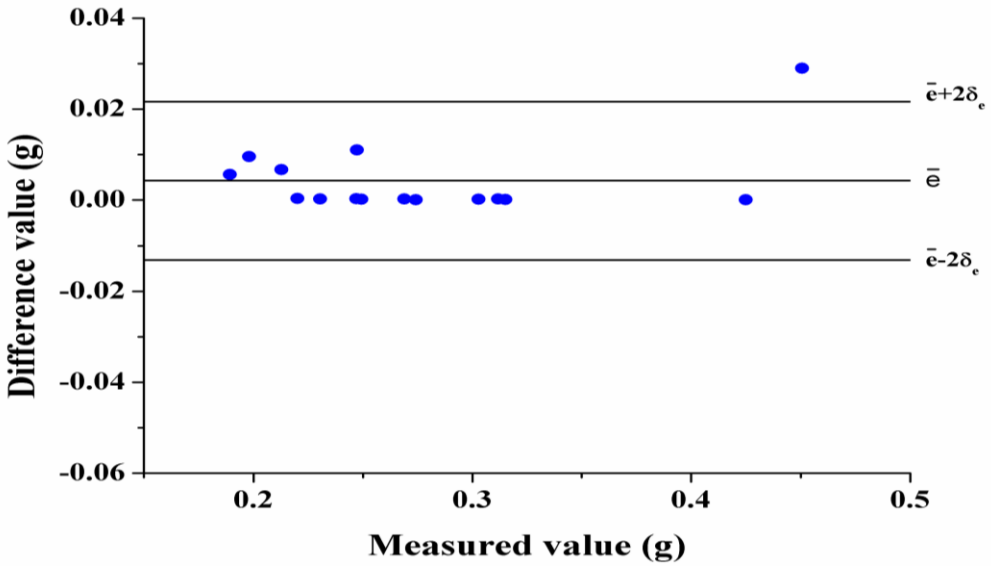

Figure 2. Statistical distribution of differences calculated by SVR-LOOCV models for Cu coating mass.

It can be seen from Figure 3 that the high amount of Cu coating mass appears in the region of low temperature range (60 to 65°C) and a moderate pH range (8 to 9). The Cu coating mass appears to have a clear second-degree parabola relation with the pH value under the above-mentioned condition. When the temperature further rises above 65°C, the influence of temperature and pH value on the Cu coating mass is less obvious.

The effective tendency of temperature and Ni^{2+} concentration on Cu coating mass as shown in Figure 4 is quite similar to that showed in Figure 3. It is obvious in Figure 4 that, when the temperature varies in the range from 60 to 70°C, the Cu coating mass would increase first and then would decrease with the Ni^{2+} concentration increasing from 1 to 3 g/L, but the Cu coating mass tend to be kept in a lower range of 0.25 to 0.3 g after the temperature is over 70°C. Previous findings (Zhang et al., 2010) showed that Cu coating mass appears a trend from little fluctuation at 65 to 70°C to slowly increase at 70 to 75°C, subsequently, increased rapidly after temperature rise to over 75°C, and reached its maximum value in the range of 75 to 85°C. Our modeling result reveals that the

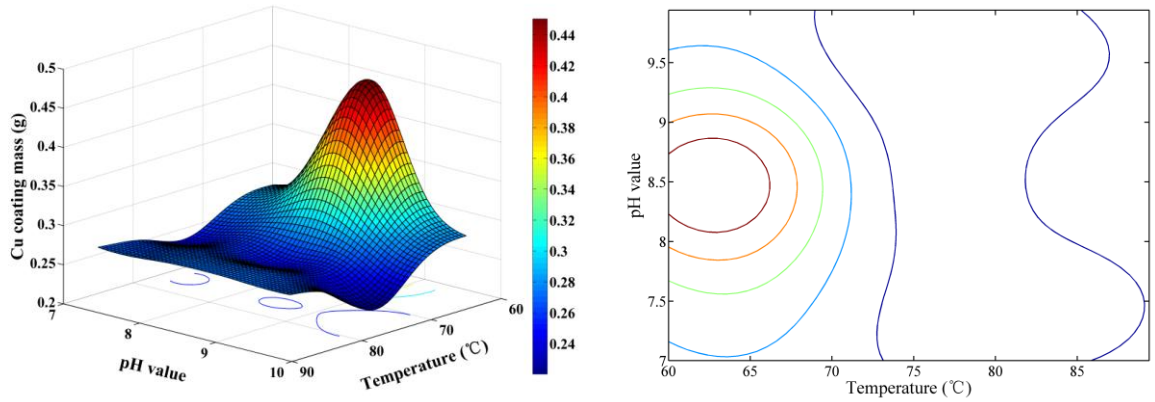

Figure 3. Interaction effect of pH value and temperature on the Cu coating mass with Ni^{2+} concentration = 1.99 g/L.

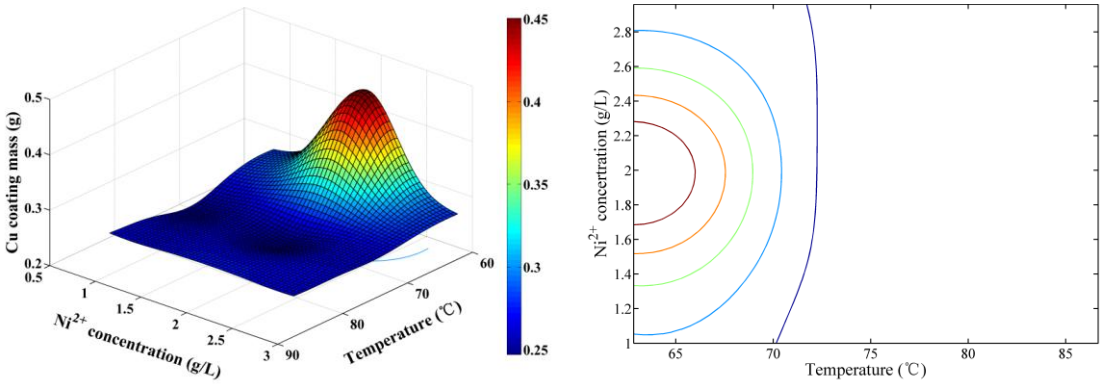

Figure 4. Interaction effect of Ni^{2+} concentration and temperature on the Cu coating mass with pH value = 8.5.

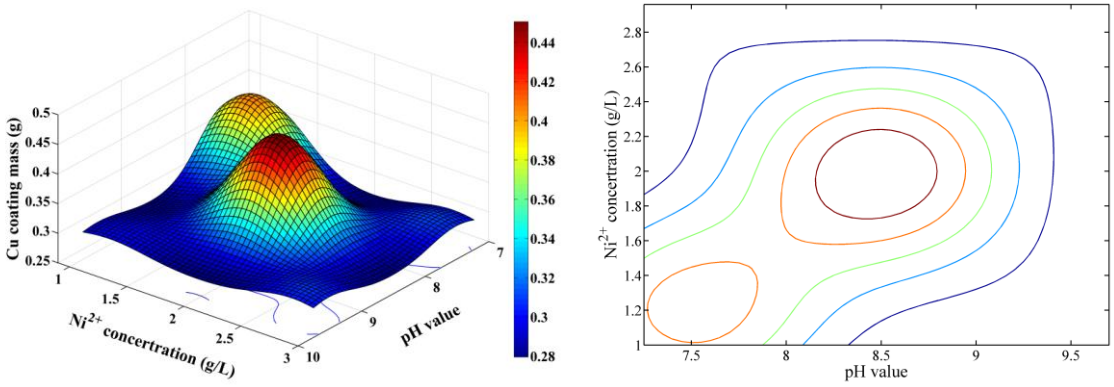

Figure 5. Interaction effect of Ni^{2+} concentration and pH value on the Cu coating mass with temperature = 62.83ºC.

peak amount of Cu coating emerges ahead of temperature reaching 70°C. This can be understood, because with temperature rising, the rough micropores formed on the surface of precipitate would obstruct the Cu coating (Zhang et al., 2010).

It can be viewed from Figure 5 that a peak amount of Cu coating mass emerges in the region of pH value from 7 to 7.5 and Ni^{2+} concentration from 1 to 1.4 g/L, and then another higher peak value presents with pH value increasing from 8.3 to 8.7 and Ni^{2+} concentration increasing

from 1.8 to 2.2 g/L. Whereafter, the Cu coating mass would drop to a lower range from 0.28 to 0.32 g accompanied with pH value or Ni^{2+} concentration increasing. This is because an overdose of OH^- would promote the generation of Cu_2O, which would prevent the Cu ions from coating, and when the proportion of Ni^{2+}/Cu is too large, the stability of electrolyte would be destroyed, which would slowdown the reaction of electroless plating (Zhang et al., 2010; Ishikawa et al., 1995).

Zhang et al. (2007, 2010) found out from their previous experiment that Cu coating can efficiently improve the discharge capacity and cycle stability of the coated hydrogen storage alloy, and a proper amount of Cu coating mass could achieve the maximum discharge capacity. It is noticed that the less the coated mass, the greater the maximum discharge capacity. Thus, the 3D changing tendency of coating mass on various plating conditions deduced via the created SVR model is helpful for the relevant experiment.

Conclusion

In this study, an empirical model for quantitative prediction of Cu coating mass on the surface of AB_5-type hydrogen storage alloy was set up via support vector regression combined with particle swarm optimization for its parameter optimization. The accuracy and reliability of the established mathematical model was tested by leave-one-out cross validation. The predicted results of SVR were also compared with those of the second-order polynomial model. It was found out by statistics that the coating amounts predicted by SVR models are more consistent with experimental results than those of the second-order polynomial model. These results demonstrate that the SVR model consistently possesses excellent simulation and generalization ability than traditional polynomial nonlinear regression. According to the established SVR model, the interaction effect of different experimental factors on the Cu coating mass was further investigated. The optimal experimental parameters can be determined according to the SVR model and three-dimensional profile. These suggest that the SVR model can be used to assist in experiment design, and optimize the process of electroless copper plating with available optimal process parameters.

ACKNOWLEDGEMENTS

This work was supported by the Fundamental Research Funds for the Central Universities (CDJXS10101107), the Program for New Century Excellent Talents in Universities of China (NCET-07-0903), the Scientific Research Foundation for the Returned Overseas Chinese Scholars of Ministry of Education, China (2008101-1) and the Natural Science Foundation of Chongqing, China (CSTC2006BB5240).

REFERENCES

Bland JM, Altman DG (1986). Statistical-methods for assessing agreement between 2 methods of clinical measurement. Lancet, 1(8476): 307-310.

Cai CZ, Han LY, Ji ZL, Chen X, Chen YZ (2003a). SVM-Prot: Web based support vector machine software for functional classification of a protein from its primary sequence. Nucleic Acids Res., 31(13): 3692-3697.

Cai CZ, Wang WL, Chen YZ (2003b). Support vector machine classification of physical and biological datasets. Int. J. Mod. Phys. C, 14(5): 575-585.

Deng C, Shi PF, Zhang S (2006). Effect of surface modification on the electrochemical performances of $LaNi_5$ hydrogen storage alloy in Ni/MH batteries. Mater. Chem. Phys., 98(2-3): 514-518.

Dong ZW, Wu YM, Ma LQ, Shen XD, Wang LM (2010). Electrochemical properties of $(La_{1-x}Ti_x)_{0.67}Mg_{0.33}Ni_{2.75}Co_{0.25}$ (x=0-0.20, at%) hydrogen storage alloys. Mater. Res. Bull., 45(3): 256-261.

Feng F, Northwood DG (2004). Effect of surface modification on the performance of negative electrodes in Ni/MH batteries. Int. J. Hydrog. Energy, 29(9): 955-960.

Hu WK, Noreus D (2010). Lab-size rechargeable metal hydride-air cells. J. Power Sources, 195(17): 5810-5813.

Ishikawa M, Enomoto H, Matsuoka M, Iwakura C (1995). Effect of some factors on electrodeposition of nickel-copper alloy from pyrophosphate-tetraborate bath. Electrochim. Acta 40(11): 1663-1668.

Kennedy J, Eberhart R (1995). Particle swarm optimization. In: Proc. IEEE Int. Conf. Neural Networks, pp. 1942-1948.

Lei YQ, Li ZP, Chen CP, Wu J, Wang QD (1991). The cycling behavior of misch metal-nickel-based metal hydride electrodes and the effects of copper plating on their performance, J. Less-Common Met., 172: 1265-1272.

Malinova T, Guo ZX (2004). Artificial neural network modelling of hydrogen storage properties of Mg-based alloys, Mater. Sci. Eng., A 365(1-2): 219-227.

Matsuoka M, Asai K, Asai K, Fukumoto Y, Iwakura C (1993). Electrochemical characterization of surface-modified negative electrodes consisting of hydrogen storage alloys, J. Alloys Compd., 192(1-2): 149-151.

Ozaki T, Kanemoto M, Kakeya T, Kitano Y, Kuzuhara M, Watada M, Tanase S, Sakai T (2007). Stacking structures and electrode performances of rare earth-Mg-Ni-based alloys for advanced nickel-metal hydride battery. J. Alloys Compd., 446-447: 620-624.

Raju M, Ananth MV, Vijayaraghavan L (2009). Influence of electroless coatings of Cu, Ni-P and Co-P on $MmNi_{3.25}Al_{0.35}Mn_{0.25}Co_{0.66}$ alloy used as anodes in Ni-MH batteries. J. Alloys Compd., 475(1-2): 664-671.

Schlapbach L, Züttel A (2001). Hydrogen-storage materials for mobile applications. Nature, 414(6861): 353-358.

Shen WZ, Han SM, Li Y, Song JZ, Tong Q (2010). Study on surface modification of AB_5-type alloy electrode with polyaniline by electroless deposition. Electrochim. Acta, 56(2): 959-963.

Singh RK, Lototsky MV, Srivastava ON (2007). Thermodynamical, structural, hydrogen storage properties and simulation studies of P-C isotherms of $(La, Mm)Ni_{5-y}Fe_y$. Int. J. Hydrog. Energy, 32(14): 2971-2976.

Thomas JE, Castro BE, Real S, Visintin A (2008). Behavior prediction of metal hydride electrodes in operation used in alkaline batteries. Int. J. Hydrog. Energy, 33(13): 3475-3479.

Tliha M, Khaldi C, Mathlouthi H, Lamloumi J, Percheron-Guegan A (2007). Electrochemical investigation of the iron-containing and no iron-containing AB_5-type negative electrodes. J. Alloys Compd., 440(1-2): 323-327.

Vapnik V (1995). The nature of statistical learning theory. Springer, New York., pp. 181-190.

Wang GL, Cai CZ, Pei JF, Zhu XJ (2011). Prediction of thermal conductivity of polymer-based composites by using support vector regression. Sci. China Phys. Mech. Astron., 54(5): 878-883.

Wei XD, Zhang P, Dong H, Liu YN, Zhu JW, Yu G (2008). Electrochemical performances of a Co-free $La(NiMnAlFe)_5$ hydrogen storage alloy modified by surface coating with Cu. J. Alloys Compd.,

458(1-2): 583-587.
Wen YF, Cai CZ, Liu XH, Pei JF, Zhu XJ, Xiao TT (2009). Corrosion rate prediction of 3C steel under different seawater environment by using support vector regression. Corros. Sci., 51(2): 349-355.
Yan DY, Sun YM, Suda S (1995). Surface properties of the F-treated ZrTiVNi alloy. J. Alloys Compd., 231(1-2): 387-391.
Yoshida H, Kawata K, Fukuyama Y, Takayama S, Nakanishi Y (2000). A particle swarm optimization for reactive power and voltage control considering voltage security assessment. IEEE Trans. Power Syst., 15(4): 1232-1239.
Yu XB, Wu Z, Huang TS (2009). Improved electrochemical performance of BCC alloy by Ni addition and surface modification with AB_5 alloy. J. Alloys Compd., 476(1-2): 787-790.
Zhang B, Wu WY, Yin SH, Li SW, Luo Y, Bian X, Tu GF (2010). Process optimization of electroless copper plating and its influence on electrochemical properties of AB_5-type hydrogen storage alloy. J. Rare Earths, 28(6): 922-926.
Zhang YH, Ren HP, Li BW, Dong XP, Cai Y, Wang XL (2007). Effect of rapid quenching on the microstructures and electrochemical characteristics of $La_{0.7}Mg_{0.3}Ni_{2.55-x}Co_{0.45}Al_x$ (x=0-0.4) electrode alloys. Mater. Charact., 58(7): 637-644.